Supplementary Information

Enhanced Luminol Chemiluminescence with Oxidase-like Activity of $NiOOH/Ni(OH)_2$ Nanoflakes for the Sensitive Detection of Mn^{2+}

Microchimica Acta

Jiaqian Qi, Yang Chen, Jing Chen, Funan Chen*

School of Chemistry and Chemical Engineering, Southwest University, Chongqing, 400715, China.

* Corresponding author；

E-mail: chenfn@swu.edu.cn

Chemicals

Nickel(II) sulfate hexahydrate, potassium persulfate, luminol, sodium hydroxide, p-benzoquinone, sodium azide, thiourea, manganese(II) sulfate, sodium chloride, potassium chloride, silver chloride, calcium chloride, barium nitrate, zinc nitrate hexahydrate, chromium(III) chloride hexahydrate, mercury(II) chloride, lead(II) nitrate, cadmium nitrate tetrahydrate, iron(III) chloride hexahydrate, and 3,3',5,5'-tetramethylbenzidine were all of analytical grade and purchased from Chongqing Titan New Chemical Co., Ltd. Deionized water was used throughout the experiments. Tap water was collected from the laboratory faucet, and lake water was obtained from Chongde Lake at Southwest University in Chongqing.

Instruments

Transmission electron microscope (TEM) images were captured using a FEI TF20 (Thermo fisher, USA). An X' Pert PRO diffractometer (Panalytical, Netherlands) was used to analyze the powder using X-ray diffraction (XRD). A Nicolet IS5 system (Thermo Fisher, USA) was used to measure the Fourier transform infrared (FT-IR) spectrum. The X-ray photoelectron spectra (XPS) spectrum data were detected using the Thermo Scientific K-Alpha (Thermal Electron, USA). Chemiluminescence signals were detected by an ultra-weak BPCL analyser (Xi'an Remax Company, Xi'an, China). The CLspectrum was tested when turning off the xenon lamp on the FS5 fluorescence spectrophotometer (Edinburgh Instruments,UK). An UV-2700 spectrometer (Shimadzu, Japan) was used to record ultraviolet-visible (UV-vis) absorption spectroscopy

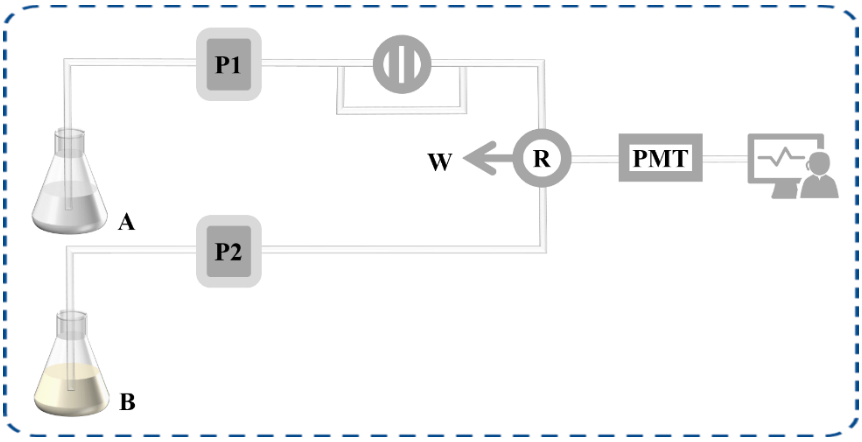

Fig. S1 Schematic diagram of the flow injection chemiluminescence system in this work. A: $NiOOH/Ni(OH)_2$ NFs solution (30 $\mu g \cdot mL^{-1}$), B: alkaline luminol solution (0.60 $mmol \cdot L^{-1}$, containing 0.02 $mol \cdot L^{-1}$ NaOH), P: peristaltic bump; R: reaction coil; W: waste; PMT: photomultiplier tube, high voltage: 650 V.

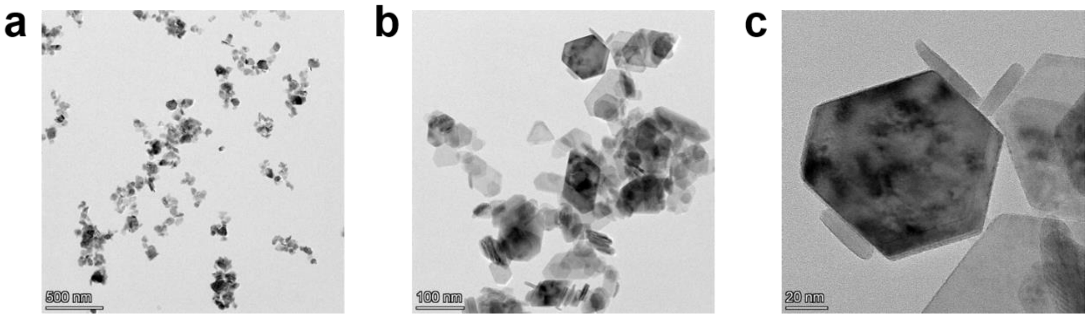

Fig. S2 500 nm **(a)**, 100 nm **(b)**, 20 nm **(c)** TEM image of $NiOOH/Ni(OH)_2$ NFs

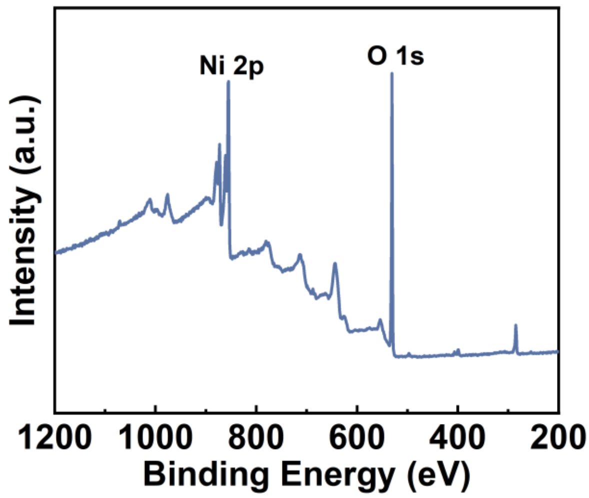

Fig. S3 XPS survey spectrum of $NiOOH/Ni(OH)_2$ NFs

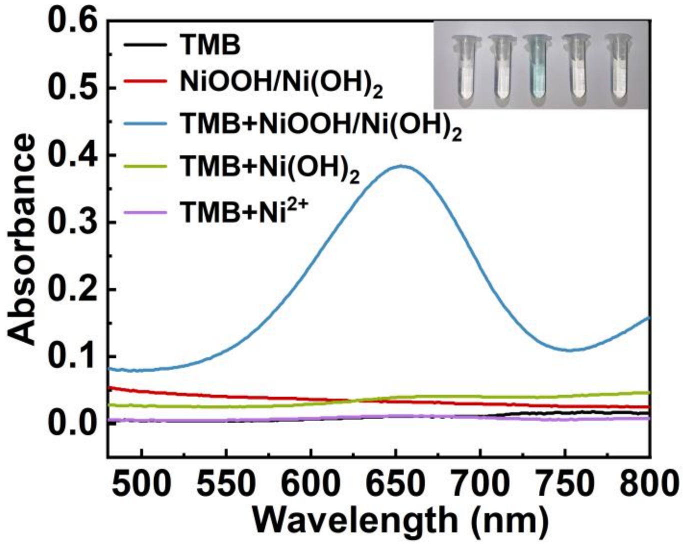

Fig. S4 UV-vis absorption spectra of TMB (black curve), $NiOOH/Ni(OH)_2$ NFs (red curve), TMB+ $NiOOH/Ni(OH)_2$ NFs (blue curve), TMB+ $Ni(OH)_2$ (green curve), TMB+Ni^{2+} (purple curve). The inset: from left to right, these solutions are shown in natural light

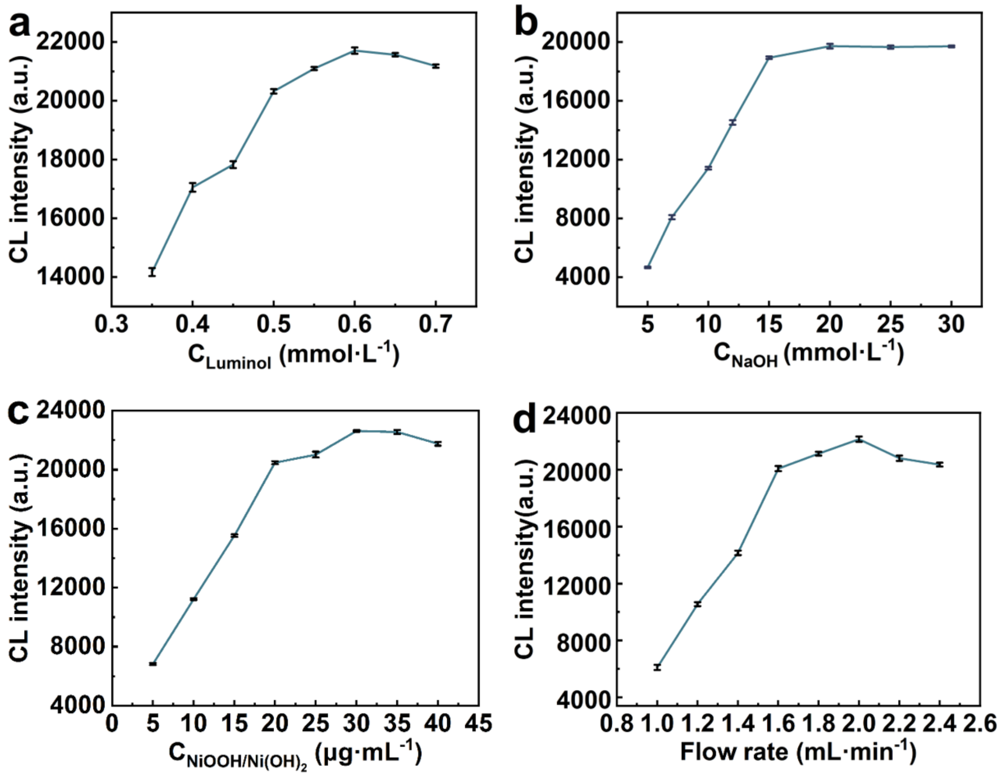

Fig. S5 Effects of concentrations **(a)** luminol, **(b)** NaOH, **(c)** $NiOOH/Ni(OH)_2$ NFs, **(d)** the flow rate of peristaltic pump on CL intensity of luminol-$NiOOH/Ni(OH)_2$ NFs system

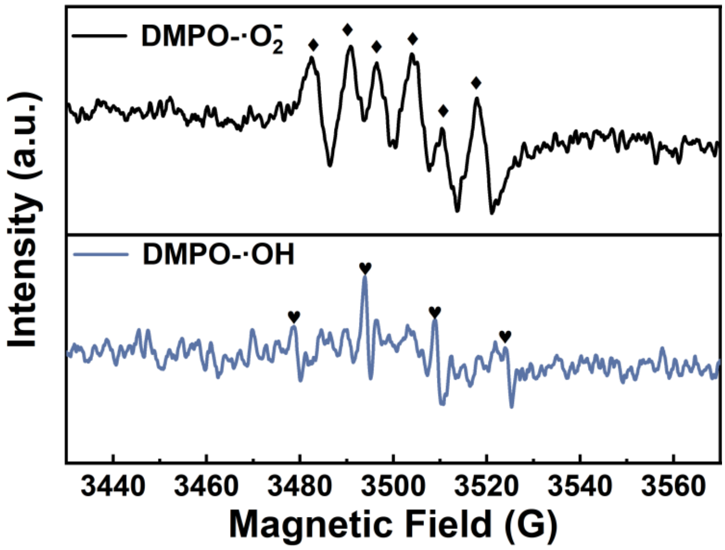

Fig. S6 ESR spectra of adduct DMPO-·O_2^- and DMPO-·OH of luminol- $NiOOH/Ni(OH)_2$ NFs

Table S1 Comparison of the constructed CL sensor based on $NiOOH/Ni(OH)_2$ NFs with other reported methods for detecting Mn^{2+} in water samples.

Materials	Methods	Linear range ($\mu mol \cdot L^{-1}$)	LOD ($\mu mol \cdot L^{-1}$)	Reference
TCPP-GO [a]	Fluorescence	25–270	1.80	[1]
KBNCDs [b]	Fluorescence	5–25	1.20	[2]
NAC2 [c]	Fluorescence	0–40	0.75	[3]
ALC/PQ-2 [d]	Colorimetry	0–40	6.95	[4]
MNA-MA-AgNPs [e]	Surface-enhanced Raman Spectroscopy	10–100	4.00	[5]
$NiOOH/Ni(OH)_2$	Chemiluminescence	1–30	0.60	This work

[a] Meso-tetrakis(4-carboxyphenyl)porphyrin-graphene oxide

[b] Kentucky bluegrass nitrogen-doped carbon dots

[c] Naphthalimide derivatives with *n*-dodecyl[-$(CH_2)_{11}CH_3$]

[d] alizarin complexone/ poly[bis(2-chloroethyl)ether-alt-1,3-bis[3-(dimethylamino)propyl]urea]

[e] 6-mercaptonicotinic acid-melamine-silver nanoparticles

Table S2 Detection of Mn^{2+} in tap water and lake water

Sample	Add ($\mu mol \cdot L^{-1}$)	Found ($\mu mol \cdot L^{-1}$, n=3) [a]	Recovery (%)	RSD (%)
Tap water	0	—	—	—
	5	4.85±0.12	96.92	2.57
	15	15.43±0.20	102.86	1.32
	25	24.73±0.40	98.94	1.60
Lake water	0	—	—	—
	5	5.03±0.18	100.51	3.58
	15	15.36±0.39	102.42	2.54
	25	24.39±0.34	97.54	1.38

[a] Mean ± standard deviation (n=3)

Reference

1. Rayati S, Farahani YD, Ghasemi JB (2024) Surface decorated graphene oxide with porphyrin: A promising on-off sensor for Mn^{2+} ions detection in aqueous media. J Mol Struct 1315:138897. https://doi.org/10.1016/j.molstruc.2024.138897

2. Krishnaiah P, Atchudan R, Perumal S, et al (2022) Utilization of waste biomass of *Poa pratensis* for green synthesis of n-doped carbon dots and its application in detection of Mn^{2+} and Fe^{3+}. Chemosphere 286:131764. https://doi.org/10.1016/j.chemosphere.2021.131764

3. Nie W, Yang J, Wu J, Hu L (2022) Synthesis and photophysical properties of vice-like 1,8-naphthalimide fluorescent sensor for sensitive detection of Mn^{2+} and Zn^{2+}. J Photochem Photobiol Chem 430:113951. https://doi.org/10.1016/j.jphotochem.2022.113951

4. Shimizu M, Aikawa S, Fukushima Y (2023) Colorimetric Probe for Mn^{2+} Using a Mixture of an Anionic Dye and a Cationic Polyelectrolyte in an Aqueous Solution. J Fluoresc 33:1367–1373. https://doi.org/10.1007/s10895-023-03148-9

5. Chen Q, Tang J, Huang Z, et al (2023) SERS scaffold based on silver nanoparticles with multi-ingredient heavy metal ligands for the determination of Mn(II). Colloid Polym Sci 301:949–956. https://doi.org/10.1007/s00396-023-05116-y